agronomy

MDPI

*Article*

# The Contribution of Microbial- and Plant-Derived Carbon to Soil Organic Carbon Fractions and Stability Under Manure Application Combined with Straw Incorporation

**Yunjie Wen [1,2], Xian Liu [1,3], Na Yang [4], Yongping Li [1,2] and Jiancheng Zhang [4,*]**

[1] Shanxi Institute of Organic Dryland Farming, Shanxi Agricultural University, Taiyuan 030031, China; wenyunjie@sxau.edu.cn (Y.W.); lx0305619@163.com (X.L.); woshiliyongping@163.com (Y.L.)
[2] National Agricultural Environment Jinzhong Observation Experiment Station, Jinzhong 030801, China
[3] College of Resources and Environment, Shanxi Agricultural University, Jinzhong 030801, China
[4] Cotton Research Institute, Shanxi Agricultural University, Yuncheng 044000, China; yn1629@163.com
* Correspondence: zhangjc@126.com

**Abstract:** The integration of manure and straw substantially affects soil organic carbon (SOC) dynamics, transformation, and long-term stabilization in agricultural systems. Dissolved organic carbon (DOC), particulate organic carbon (POC), and mineral-associated organic carbon (MOC) are the three main components of the SOC pool, each influencing soil carbon dynamics and nutrient cycling. Current research gaps remain regarding how combined fertilization practices affect the inputs of plant-originated and microbe-derived carbon into SOC pools and stability mechanisms. Our investigation measured SOC fractions (DOC, POC, MOC), SOC mineralization rate (SCMR), microbial necromass carbon, lignin phenols, enzyme activities, and microbial phospholipid fatty acids (PLFAs) over a long-term (17 years) field experiment with four treatments: mineral fertilization alone (CF), manure-mineral combination (CM), straw-mineral application (CS), and integrated manure-straw-mineral treatment (CMS). The CMS treatment exhibited notably elevated levels of POC (7.42 g $kg^{-1}$), MOC (10.7 g $kg^{-1}$), and DOC (0.108 g $kg^{-1}$), as well as a lower SCMR value (1.85%), compared with other fertilization treatments. Additionally, the CMS treatment stimulated the buildup of both bacterial and fungal necromass while enhancing the concentrations of ligneous biomarkers (vanillin, syringyl, and cinnamic derivatives), which correlated strongly with the elevated contents of fungal and bacterial PLFAs and heightened activity of carbon-processing enzymes (α-glucosidase, polyphenol oxidase, cellobiohydrolase, peroxidase, N-acetyl-β-D-glucosidase). Furthermore, fungal and bacterial microbial necromass carbon, together with lignin phenols, significantly contributed to shaping the composition of SOC. Through random forest analysis, we identified that the contents of bacterial and fungal necromass carbon were the key factors influencing DOC and MOC. The concentrations of syringyl phenol and cinnamyl phenols, and the syringyl-to-cinnamyl phenols ratio were the primary determinants for POC, while the fungal-to-bacterial necromass carbon ratio, as well as the concentrations of vanillyl, syringyl, and cinnamyl phenols, played a critical role in SCMR. In conclusion, the manure combined with straw incorporation not only promoted microbial growth and enzyme activity but also enhanced plant- and microbial-derived carbon inputs. Consequently, this led to an increase in the contents and stability of SOC fractions (DOC, POC, and MOC). These results suggest that manure combined with straw is a viable strategy for soil fertility due to its improvement in SOC sequestration and stability.



Academic Editor: Nikolaos Monokrousos

Received: 13 May 2025
Revised: 6 June 2025
Accepted: 9 June 2025
Published: 11 June 2025

**Citation:** Wen, Y.; Liu, X.; Yang, N.; Li, Y.; Zhang, J. The Contribution of Microbial- and Plant-Derived Carbon to Soil Organic Carbon Fractions and Stability Under Manure Application Combined with Straw Incorporation. *Agronomy* **2025**, *15*, 1424. https://doi.org/10.3390/agronomy15061424

**Keywords:** organic amendments; particulate organic carbon; mineral-associated organic carbon; carbon mineralization rate; microbial necromass carbon; lignin phenol

## 1. Introduction

The dynamics of soil organic carbon (SOC) directly influence soil fertility maintenance, agricultural productivity enhancement, and global carbon balance regulation [1]. Amid escalating climate challenges and food demand pressures, improving soil carbon sequestration through agricultural interventions has emerged as a global scientific priority. Dissolved organic carbon (DOC), particulate organic carbon (POC), and mineral-associated organic carbon (MOC) are the main components of SOC. DOC, in liquid form, is easily decomposed by microbes and aids nutrient availability. POC, linked to soil particles, consists of partially decomposed plant and animal matter, enhancing soil structure and slowing decomposition. MOC, tightly bound to minerals, decomposes very slowly, contributing to long-term carbon storage and soil fertility [2]. Straw incorporation combined with manure application, as typical methods for regulating carbon input, can alter the composition of the soil carbon pool by introducing exogenous organic matter. Nevertheless, critical knowledge gaps persist regarding the long-term partitioning behavior and stabilization processes of various SOC fractions under long-term effects.

Crop residues rich in cellulose and hemicellulose, and their incorporation into the field, can substantially enhance soil POC. However, this process is constrained by the slow degradation rate of lignin phenolic compounds [3]. In contrast, humified substances in manure tend to bind more readily with mineral surfaces, forming MOC, which exhibits significantly higher chemical stability compared to free components [2,4]. Recent research indicated that combining these two methods can enhance the carbon pool structure by providing complementary carbon inputs [5,6]. Straw offered labile carbon for quick cycling, while organic fertilizers added stable components that extended carbon retention [7]. However, long-term field trials are needed to confirm the effects of this synergy on carbon stabilization.

Microbial metabolites and plant-derived compounds are key precursors for SOC formation. Microbial necromass carbon, including amino sugars, can make up 40–60% of SOC, reflecting microbial-mediated carbon transformation efficiency [8,9]. Lignin phenols, key components of plant cell walls, and their oxidized derivatives (e.g., vanillic acid and p-hydroxybenzoic acid) can form covalent bonds with minerals, affecting the chemical stability of MOC [10,11]. In agricultural ecosystems under different fertilization regimes, microbial necromass carbon and lignin phenols differently affected SOC [12–14]. For instance, nitrogen addition enhanced microbial necromass dynamics, particularly influencing MOC through increased amino sugar accumulation [15,16]. In contrast, high straw-input systems showed an 88.7% increase in ligneous component concentrations and a 74.2% increase in SOC contributions [17]. The distinct chemical properties and decomposition rates of manure and crop residues regulated microbial metabolism, necromass accumulation, and lignocellulose degradation, ultimately determining SOC composition. Current research has predominantly focused on microbial necromass and lignin independently, resulting in limited understanding of their interactive effects on the dynamics and stabilization mechanisms of SOC fractions.

While many short-term experiments have documented the carbon sink effects of straw or organic fertilizers, long-term data remain limited. Research is especially lacking in two critical areas: (1) the growth and decline patterns of POC and MOC, as well as the stabilization mechanisms of SOC over decadal scales; and (2) the differential contributions of microbial necromass carbon and lignin phenols to SOC fractions and stability. To address

these gaps, this study employed a 17-year field observation experiment to elucidate: (1) the regulatory pathways through which long-term straw incorporation combined with manure application affects SOC fractions and stability; and (2) the functional partitioning and synergistic mechanisms of microbial necromass carbon and lignin phenols in shaping SOC fractions and stability. These insights will enhance theoretical frameworks for optimizing farmland carbon management and support evaluations of agricultural soil carbon sink potential under global change.

## 2. Materials and Methods

### *2.1. Experimental Site and Design*

The experiment was conducted at the Shuitou Experimental Base of Shanxi Agricultural University, located in Yuncheng City, Shanxi Province. This region experiences a mean annual temperature of 13.4 °C with 525 mm of precipitation, featuring 2040 sunshine hours and 212 frost-free days annually. The soil in the experimental area is classified as Calcaric-Fluvic Cambisol [18] with initial topsoil properties showing 10.9 g $kg^{-1}$ organic carbon, 89.6 mg $kg^{-1}$ available N, 13.1 mg $kg^{-1}$ available P, 170 mg $kg^{-1}$ exchangeable K, and alkaline pH of 8.4. The experiment commenced in 2007 and comprised four fertilization treatments: mineral-only fertilization (CF), manure-mineral combination (CM), straw-mineral integration (CS), and full manure-straw-mineral treatment (CMS). Each experimental plot measured 3 m in width and 20 m in length, encompassing a total area of 60 square meters, with three replicates assigned to each treatment. Twelve replications within four plots were randomly arranged. A 0.5 m protective row was established outside the plots to minimize the impact of edge effects on the experiment. The chemical fertilizers utilized in the study were urea, containing 46% nitrogen (N), and double superphosphate, containing 46% phosphorus pentoxide ($P_2O_5$), which were used as seed fertilizers and applied together with the seeds in October. The application rates were 360 kg per hectare for urea and 326 kg per hectare for double superphosphate. The organic fertilizer used was decomposed chicken manure, which contained 21% organic matter, 1.71% total nitrogen, and was applied at an annual rate of 15 tonnes per hectare in October before planting wheat for both the CM and CMS treatments. Following the wheat harvest in June each year, the straw from the CS and CMS treatments was completely crushed and reincorporated into the field, whereas the straw from the CF and CM treatments was removed.

### *2.2. Sample Collection*

Following the wheat harvest in late June 2024, composite soil samples were collected from the surface layer (0–20 cm) using a five-point sampling method and immediately transported to the laboratory. All extraneous materials, such as stones, roots, and straw residues, were meticulously removed by manual extraction. A subset of the samples was cryopreserved at −80 °C for subsequent analysis of soil enzyme activity and microbial community composition, typically analyzed within one month. Another portion was naturally air-dried, sieved through a 2 mm mesh for the determination of organic carbon fractions, and further sieved through a 0.15 mm mesh for the analysis of organic carbon, lignin phenols, and amino sugar compounds.

### *2.3. SOC Mineralization Rate*

Initially, 10 g fresh soil samples were adjusted to a moisture content equivalent to 60% of their water-field capacity, which was determined using the ring knife method (Method S1). The samples were then transferred into 500 mL culture flasks, each equipped with a small beaker containing 10 mL of 0.5 mol $L^{-1}$ NaOH solution (Sinopharm Chemical Reagent Co., Ltd., Shanghai, China) to absorb $CO_2$ released during incubation. Four

replicates were prepared for each soil sample, along with control flasks devoid of soil. The flasks were sealed and incubated in a dark environment at 25 °C. On days 3, 6, 9, 12, 15, 18, 21, 24, 27, and 30, the beakers containing NaOH were removed, and 20 mL of 1 mol $L^{-1}$ $BaCl_2$ solution (Sinopharm Chemical Reagent Co., Ltd., Shanghai, China) along with two drops of phenolphthalein indicator were added. The mixture was then titrated with 0.2 mol $L^{-1}$ HCl solution (Sinopharm Chemical Reagent Co., Ltd., Shanghai, China) to quantify $CO_2$ emissions. The NaOH solution was replaced after each sampling event. To ensure sufficient oxygen supply, all culture flasks were aerated for 30 min at each sampling interval. The weighing method was employed to standardize the soil moisture content across all soil samples. Additionally, the initial weight of the soil was maintained by periodically adding distilled water as necessary [5].

SOC mineralization amount (SMA) calculation:

$$SMA = C_{HCl} \times (V_0 - V) \times \frac{22}{0.03}$$

SOC cumulative mineralization amount (CMA) calculation:

$$CMA = \sum_{i=1}^{n} SMA$$

SOC mineralization rate (SCMR) calculation:

$$SCMR = \frac{CMA}{SOC}$$

Among these parameters, $C_{HCl}$ represents the concentration of the titrated HCl solution, which was 0.2 mol $L^{-1}$; $V_0$ and V denote the blank titration volume and the volume of HCl consumed during titration, respectively, both measured in mL; i indicates the number of sampling instances; SOC refers to the soil organic carbon content.

### *2.4. SOC Fractions*

Initially, a 20.0 g soil sample, which had been previously passed through a 2 mm mesh sieve, was combined with 100 mL of deionized water. This mixture underwent oscillation and dispersion, resulting in a supernatant that represented the dissolved organic carbon (DOC). Subsequently, 100 mL of a 0.5% sodium hexametaphosphate solution (Sinopharm Chemical Reagent Co., Ltd., Shanghai, China) was added to the remaining precipitate. Following thorough oscillation and dispersion, the resulting suspension was filtered through a 0.053 mm mesh sieve. The residue retained on the sieve was then dried in an oven set at 45 °C and weighed to determine the particulate organic carbon (POC) content. The filtrate obtained from the soil sample was also dried and weighed to ascertain the mineral-associated organic carbon (MOC) content [2]. The POC and MOC contents were determined through elemental analysis using an Elementar vario PYRO cube (vario PYRO cube, Germany)

### *2.5. Microbial Necromass Carbon*

As microbial necromass biomarkers, soil amino sugars were quantified according to established protocols [19]. Specifically, 0.5 g of air-dried soil samples were accurately weighed and hydrolyzed with 6 mol $L^{-1}$ hydrochloric acid (Sinopharm Chemical Reagent Co., Ltd., Shanghai, China) at 105 °C for 8 h under constant temperature conditions. After cooling to room temperature, the hydrolysates were supplemented with 100 μL inositol (Sinopharm Chemical Reagent Co., Ltd., Shanghai, China) as internal standard, vortex-mixed, and filtered. The clarified solutions were concentrated via rotary evaporation

(65 °C), neutralized using KOH (pH 6.6–6.8) (Sinopharm Chemical Reagent Co., Ltd., Shanghai, China), then centrifuged (4000 rpm, 10 min) for phase separation. The colloidal fractions underwent methanol solubilization and repeated centrifugation for salt removal. Purified extracts were transferred into derivatization vessels for nitrogen-assisted solvent evaporation (45 °C), resolubilized in ultrapure water, and lyophilized. Derivatization involved sequential addition of 300 μL reaction reagent with 30 min incubation at 80 °C, followed by 1 mL acetic anhydride (Sinopharm Chemical Reagent Co., Ltd., Shanghai, China) treatment for 20 min acetylation at identical temperature. Post-derivatization processing included extraction with 1 mL dichloromethane (Sinopharm Chemical Reagent Co., Ltd., Shanghai, China) and 1 M HCl (Sinopharm Chemical Reagent Co., Ltd., Shanghai, China) phase separation. The organic layers were washed with deionized water, dried under nitrogen purge (45 °C), then reconstituted in 300 μL n-hexane/ethyl acetate (1:1 $v/v$) for GC analysis. Chromatographic separation enabled quantification of glucosamine (GluN), mannosamine (ManN), galactosamine (GalN), and muramic acid (MurA). Fungal necromass carbon (FNC, g $kg^{-1}$) and bacterial necromass carbon (BNC, g $kg^{-1}$) were calculated according to the following formulas:

$$FNC = \left(\frac{GLuN}{179.17} - 2 \times \frac{MurA}{251.23}\right) \times 179.17 \times 9$$

$$BNC = MurA \times 45$$

The formulas incorporate molecular weights of GluN (179.17 g $mol^{-1}$) and MurA (251.23 g $mol^{-1}$), with coefficients 9 and 45 applied for fungal and bacterial necromass carbon conversion, respectively.

### *2.6. Lignin Phenols*

The extraction of lignin phenolic monomer substances was performed through alkaline CuO oxidation methodology [20]. Preliminary extraction removed interfering compounds including n-alkanes, alkanols, fatty acids, and steroids through sequential organic solvent treatments. Post-extraction, oxidative treatment with CuO yielded three lignin phenol categories: vanillyl (V-type), syringyl (S-type), and cinnamyl (C-type) derivatives. These analytes were derivatized with trimethylsilyl groups prior to gas chromatography-mass spectrometry (GC-MS, Agilent 7980B-5977a, America). Phenolic monomer concentrations were determined by GC-MS, with total lignin phenol content calculated through summation of V+S+C components [21]. Ratios of syringyl-to-vanillyl and cinnamyl-to-vanillyl phenols served as oxidative degradation indices, where lower values corresponded to a higher degree of oxidative degradation.

### *2.7. Soil Enzyme Activity and Phospholipid Fatty Acid*

The activities of soil enzymes, including α-glucosidase, β-glucosidase, polyphenol oxidase, cellobiohydrolase, peroxidase, and N-acetyl-β-D-glucosaminidase, were extracted using Solarbio activity detection kits and quantified using a multi-functional microplate reader (BioTek Synergy LX, Agilent, America).

Phospholipid fatty acid (PLFA) analysis [22] was implemented to characterize microbial biomass and community composition. Specifically, the procedure involved the following steps: First, 5.0 g of freeze-dried soil samples were measured, followed by phospholipid extraction with a methanol-chloroform-citric acid mixture (2:1:0.8 $v/v$). Subsequently, phospholipid isolation was performed using solid-phase extraction columns. Finally, methylation of the phospholipids was conducted using methanol, a methanol-toluene mixture, and n-hexane solutions. The resulting phospholipid fatty acids were quantitatively analyzed via gas chromatography (Agilent-6890N, America), and qualita-

tive identification was achieved using the MIDI Sherlock microbial identification system. The PLFAs were used as proxies for the biomass of total bacteria and fungi. Based on the interpretations provided in Table S1, the content of phospholipid fatty acids is given as nmol $g^{-1}$.

### *2.8. Statistical Analysis*

The one-way ANOVA (Duncan's test, $p < 0.05$) was performed to analyze the differences in organic carbon fractions, microbial residues, lignin phenols, enzyme activities, and PLFA among treatments using SPSS 24.0 software. The Pearson's correlation and Mantel's test were employed to examine the relationships between microbial necromass, lignin phenols, PLFAs, and enzyme activities using the vegan R package (version 4.3.2) [23]. Additionally, a random forest prediction model and variance partitioning analysis were conducted to evaluate the effects of microbial residues and lignin phenols on organic carbon fractions using the rfPermute R package and Canoco 5.0, respectively. In the random forest prediction model, the importance of each predictor variable is quantified by the percentage increase in mean squared error (MSE). Higher MSE% values indicate greater importance. The $R^2$ metric evaluates the model's goodness of fit, with values closer to 1 indicating higher prediction accuracy [24]. The figures were generated using Origin 2024 software.

## 3. Results

### *3.1. SOC Fraction and Stability*

Fertilization regimes exhibited significant variations in the composition and stabilization dynamics of SOC (Figure 1). Among all treatments, the CMS treatment showed the highest levels of SOC, DOC, and MOC, with values of 16.97 g $kg^{-1}$, 108.3 mg $kg^{-1}$, and 10.7 g $kg^{-1}$, respectively, significantly higher than the values observed in the CF, CM, and CS treatments. The POC content in the CMS treatment was 7.42 g $kg^{-1}$, significantly higher than that in the CF and CM treatments. Additionally, the MOC-to-POC ratio in the CMS treatment was 1.45, significantly higher than that in the CS treatment, though no significant difference was observed compared to the CF and CM treatments. The SCMR in the CMS treatment was 1.85%, which was significantly lower than the rates observed in the CF and CS treatments.

### *3.2. Microbial Necromass and Lignin Phenols*

Different fertilization treatments significantly influenced soil microbial necromass (Figure 2). The bacterial necromass carbon content in the CMS treatment was 0.66 g $kg^{-1}$, representing a significant increase of 52.0%, 19.4%, and 31.9% relative to CF, CM, and CS treatments respectively. Fungal and total microbial necromass carbon in the CMS treatment measured 5.67 and 6.34 g $kg^{-1}$, respectively, demonstrating significantly elevated levels compared to the CF and CS treatments while remaining statistically comparable to the CM treatment. The fungal-to-bacterial necromass ratio exhibited no notable variations among the CM, CS, and CMS treatments; however, both the CM and CMS treatments exhibited significantly higher ratios compared to the CF treatment.

The contents of soil lignin phenolic monomers exhibited significant variation across the different treatments (Figure 3). Specifically, the CMS treatment had vanillyl and total lignin phenol concentrations of 112.1 and 324.5 mg $kg^{-1}$ respectively, exceeding values from the CF, CM, and CS treatments. The syringyl phenol content of the CMS (144.8 mg $kg^{-1}$) and CS (134.2 mg $kg^{-1}$) treatments showed no statistical difference, though both values surpassed those of CF and CM treatments. Additionally, the cinnamyl phenol concentration in the CMS treatment was 67.6 mg $kg^{-1}$, which was also significantly higher than in the CF and CM treatments. The syringyl-to-vanillyl and cinnamyl-to-vanillyl phenol ratios

in the CMS treatment were the lowest at 1.30 and 0.60, respectively, though no significant differences were detected compared to the CF, CM, and CS treatments.

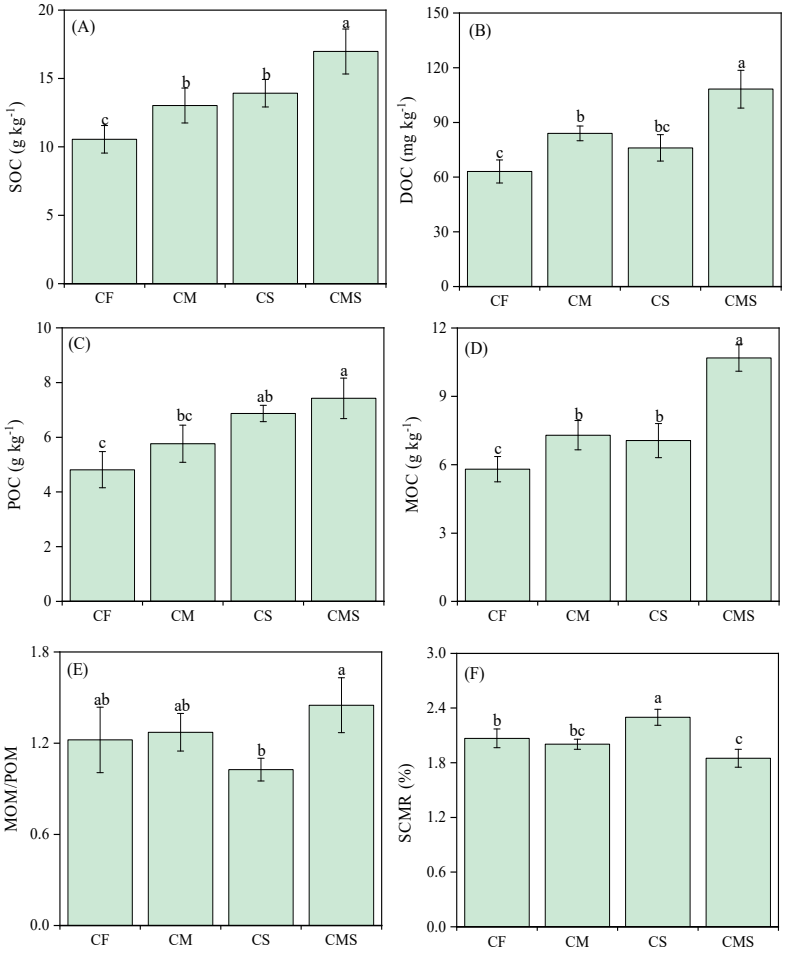


**Figure 1.** Effects of different fertilization treatments on the soil organic carbon (SOC) (**A**), dissolved organic carbon (DOC) (**B**), particulate organic carbon (POC) (**C**), mineral-associated organic carbon (MOC) (**D**), MOC-to POC ratio (MOC/POC) (**E**), and SOC mineralization rate (SCMR) (**F**). Different lowercase letters indicate significant differences between treatments ($p < 0.05$). The error line shows the standard deviation of the three repeated measurements. CF, CM, CS, and CMS indicate chemical fertilizer, manure combined with chemical fertilizer, straw returning combined with chemical fertilizer, and straw returning combined with manure and chemical fertilizer.

### *3.3. Enzyme Activity and Microbial Community Composition*

The effects of different fertilization treatments on soil enzyme activities varied significantly (Table 1). The activities of β-glucosidase and N-acetyl-β-D-glucosaminidase were consistently measured across the CMS, CS, and CM treatments, and exhibited significantly higher values compared to the CF treatment. The CMS treatment led to significantly higher α-glucosidase, polyphenol oxidase, and peroxidase activities compared to the CM and CF treatments, while exhibiting comparable levels to the CS treatment. Additionally, cellulobiase hydrolase activity in the CMS treatment was greater than that in the CS and CF treatments, yet remained statistically similar to that of the CM treatment.

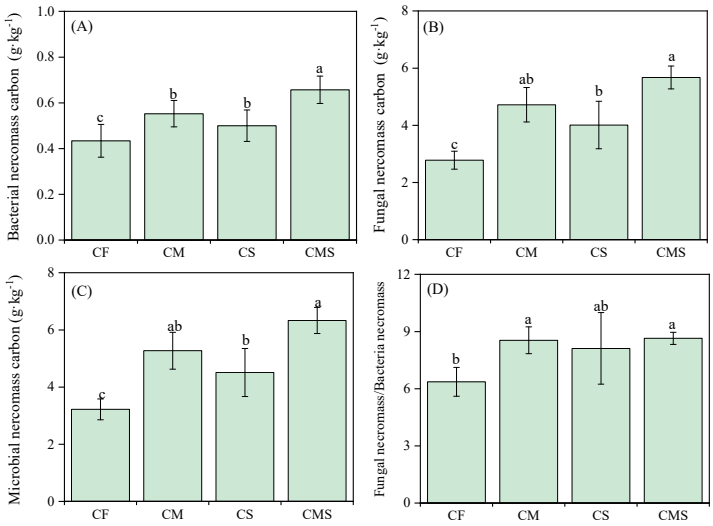


**Figure 2.** Effects of different fertilization treatments on the soil bacterial necromass carbon (**A**), fungal necromass carbon (**B**), microbial necromass carbon (**C**) contents, and fungal necromass-to-bacterial necromass carbon ratio (**D**). Different lowercase letters indicate significant differences between treatments ($p < 0.05$). The error line shows the standard deviation of the three repeated measurements. CF, CM, CS, and CMS indicate chemical fertilizer, manure combined with chemical fertilizer, straw returning combined with chemical fertilizer, and straw returning combined with manure and chemical fertilizer.

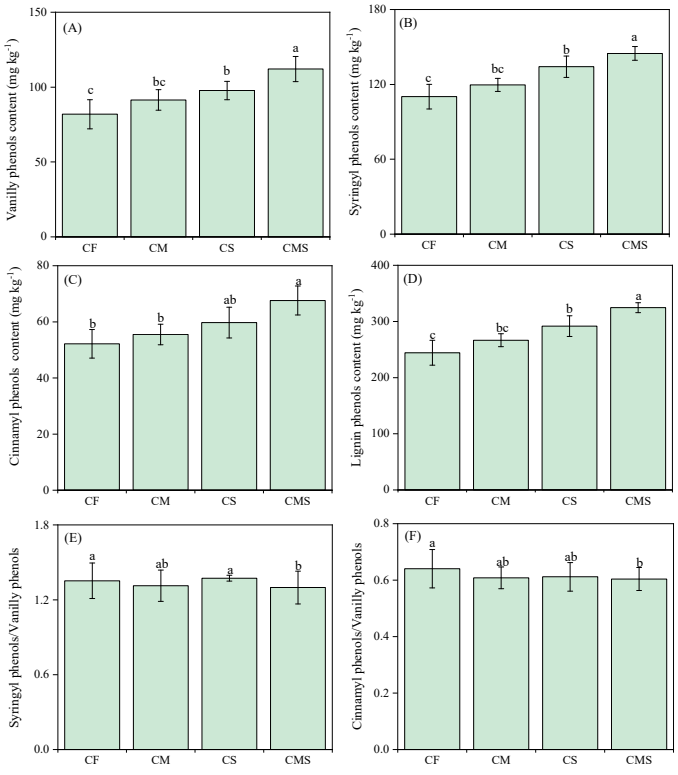


**Figure 3.** Effects of different fertilization treatments on the soil vanilly phenols (**A**), syringyl phenols (**B**), and cinnamyl phenols (**C**), lignin phenols (**D**) contents, syringyl phenols-to-vanilly phenols ratio (**E**), and cinnamyl phenols-to- vanilly phenols ratio (**F**). Different lowercase letters indicate significant differences between treatments ($p < 0.05$). The error line shows the standard deviation of the three repeated measurements. CF, CM, CS, and CMS indicate chemical fertilizer, manure combined with chemical fertilizer, straw returning combined with chemical fertilizer, and straw returning combined with manure and chemical fertilizer.

In the CMS treatment, the concentrations of total PLFAs, bacterial PLFAs, and fungal PLFAs were significantly higher than those in the CF and CS treatments, but no significant difference was detected compared to the CM treatment. Additionally, the CS treatment showed significantly greater levels of total PLFAs, bacterial PLFAs, and fungal PLFAs compared to the CF treatment. The fungal-to-bacterial PLFA ratio in the CMS treatment was the lowest at 0.20, which was significantly lower than the ratios observed in the CF and CS treatments, while no significant difference was found when compared to the CM treatment (Figure 4).

**Table 1.** Effect of different fertilization treatments on soil enzyme activity.

| Treatments | αG ($\mu mol \cdot d^{-1} \cdot g^{-1}$) | βG ($\mu mol \cdot d^{-1} \cdot g^{-1}$) | PPO ($\mu mol \cdot d^{-1} \cdot g^{-1}$) | CB ($\mu mol \cdot d^{-1} \cdot g^{-1}$) | NAG ($\mu mol \cdot d^{-1} \cdot g^{-1}$) | POD ($\mu mol \cdot d^{-1} \cdot g^{-1}$) |
|---|---|---|---|---|---|---|
| CF | 15.3 ± 1.2 c | 67.0 ± 5.9 b | 312.7 ± 12.5 b | 67.6 ± 10.5 b | 6.1 ± 2.7 b | 73.81 ± 8.97 c |
| CM | 21.7 ± 0.5 b | 95.8 ± 10.5 a | 318.1 ± 29.9 b | 78.8 ± 3.2 ab | 13.2 ± 1.9 a | 81.29 ± 7.95 bc |
| CS | 24.7 ± 2.8 ab | 103.1 ± 12.9 a | 341.5 ± 45.3 ab | 75.1 ± 4.6 b | 13.9 ± 1.4 a | 90.92 ± 6.92 ab |
| CMS | 26.6 ± 2.1 a | 99.7 ± 10.1 a | 391.9 ± 14.3 a | 87.8 ± 2.7 a | 15.7 ± 1.4 a | 97.52 ± 4.41 a |

αG, βG, PPO, CB, NAG, and POD respectively indicate α-glucosidase, β-glucosidase, polyphenol oxidase, cellobiohydrolase, N-acetyl-β-D-glucosaminidase, peroxidase. Different lowercase letters indicate significant differences between treatments ($p < 0.05$). CF, CM, CS, and CMS indicate chemical fertilizer, manure combined with chemical fertilizer, straw returning combined with chemical fertilizer, and straw returning combined with manure and chemical fertilizer.

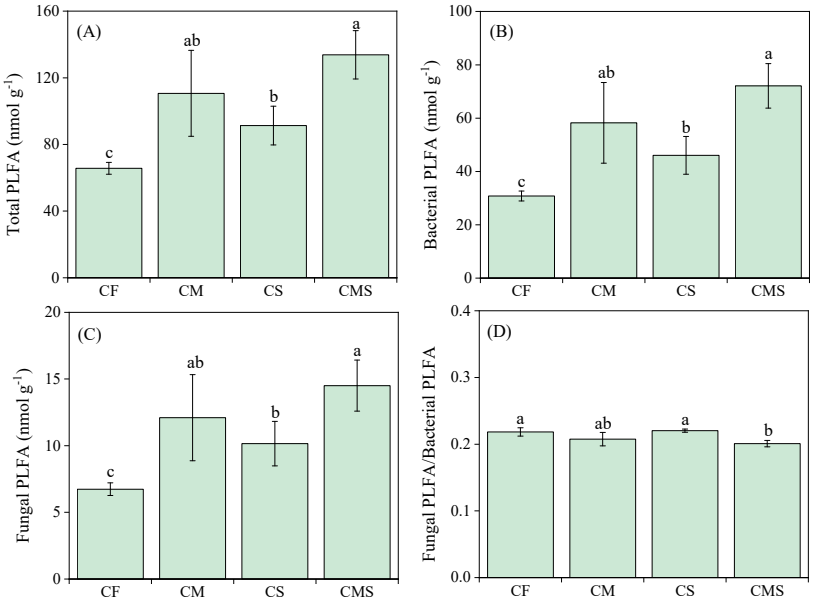


**Figure 4.** Effects of different fertilization treatments on total phospholipid fatty acid (PLFA) (**A**), bacterial PLFA (**B**), fungal PLFA (**C**), and fungal PLFA-to-bacterial PLFA ratio (**D**). Different lowercase letters indicate significant differences between treatments ($p < 0.05$). The error line shows the standard deviation of the three repeated measurements. CF, CM, CS, and CMS indicate chemical fertilizer, manure combined with chemical fertilizer, straw returning combined with chemical fertilizer, and straw returning combined with manure and chemical fertilizer.

### *3.4. Effects of Enzyme and Microorganism on Microbial Necromass and Lignin Phenols*

Pearson correlation analysis and Mantel's test were employed to investigate the interrelationships among soil microbial necromass, lignin phenols, enzyme activities, and PLFAs, as depicted in Figure 5. The analysis revealed a significant positive correlation between soil enzyme activities and microbial PLFAs. Conversely, the bacteria-to-fungi ratio demonstrated a negative correlation with soil enzyme activities, with a particularly significant association observed with cellobiohydrolase activity. Mantel's analysis further

indicated that the activities of enzymes such as α-glucosidase, β-glucosidase, peroxidase, and N-acetyl-β-D-glucosidase, along with total PLFAs, bacterial PLFAs, and fungal PLFAs, were significantly or highly significantly positively correlated with microbial necromass ($p < 0.05$, Mantel's r > 0.25). Moreover, the enzymatic activities of α-glucosidase, polyphenol oxidase, cellobiohydrolase, and peroxidase, in addition to total PLFAs, bacterial PLFAs, and fungal PLFAs, exhibited significant or extremely significant positive correlations with lignin phenols ($p < 0.05$, Mantel's r > 0.25).

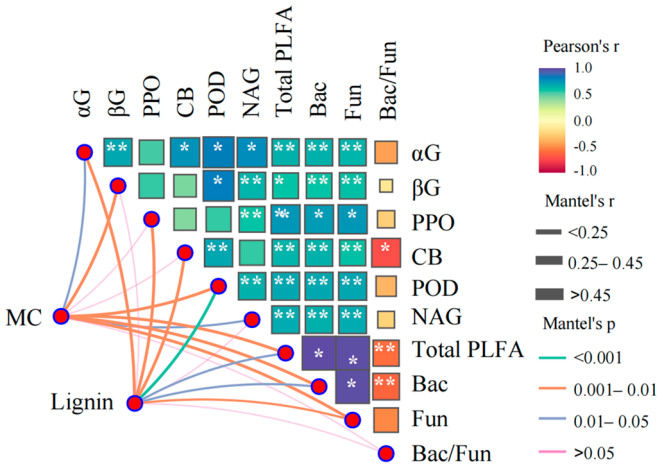


**Figure 5.** Results of correlation analysis and the Mantel analysis of microbial necromass, lignin phenols, enzymatic activity, and microbial PLFAs ($n = 12$). MC: bacterial, fungal, and total microbial necromass carbon; Lignin: vanillyl phenol, syringyl phenol, cinnamyl phenol, lignin phenol, syringyl-to-vanillyl phenol ratio, cinnamyl-to-vanillyl phenol ratio; αG: α-glucosidase; βG: β-glucosidase; PPO: polyphenol oxidase; CB: cellobiohydrolase; POD: peroxidase; NAG: N-acetyl-β-D-glucosidase; Bac: bacterial PLFAs; Fun: fungal PLFAs; Bac/Fun: bacterial-to-fungal PLFAs ratio. * and ** indicate statistically significance at $p < 0.05$ and $p < 0.01$.

### *3.5. Effects of Microbial Necromass and Lignin Phenols on SOC Fraction*

The relationships between SOC fractions, stability, microbial necromass, and lignin phenols were analyzed using Pearson's correlation (Figure 6A). It was found that bacterial, fungal, and total microbial necromass carbon, along with the fungal-to-bacterial necromass ratio, syringyl phenol, vanillyl phenol, lignin phenol, and cinnamyl phenol, demonstrated a negative correlation with SCMR, and a significantly positive or extremely significant positive correlation with POC. Furthermore, bacterial, fungal, and total microbial necromass carbon, syringyl phenol, vanillyl phenol, lignin phenol, and cinnamyl phenol showed significant or extremely significant positive correlations with both MOC and DOC. Additionally, the syringyl-to-vanillyl and cinnamyl-to-vanillyl phenol ratios were positively correlated with SCMR, while exhibiting negative correlations with the MOC, DOC, and SOC.

The influence of soil microbial necromass and lignin phenols on the SOC fractions was further examined using variance partitioning analysis (Figure 6B). This analysis demonstrated that 86.6% of the variation in SOC fractions could be attributed to microbial necromass and lignin phenols. Specifically, microbial necromass accounted for 19.9% of the variation, lignin phenols contributed 18.7%, and the combined effect of microbial necromass and lignin phenols explained 48.0% of the variation in SOC fractions.

By employing predictive analysis through the random forest model, we identified the key factors influencing SOC fractions (Figure 6C–F). Notably, in the case of DOC, bacterial necromass carbon (33.0%), total microbial necromass carbon (18.7%), and the cinnamyl-to-vanillyl phenol ratio (12.3%) were identified as the main drivers of its variation. For the POC, the syringyl phenol (15.0%), syringyl-to-vanillyl phenol ratio (15.1%), cinnamyl-to-vanillyl

phenol ratio (11.6%), fungal necromass carbon (13.2%), and cinnamyl phenol (11.1%) were found to play significant roles. The MOC was predominantly influenced by total microbial (28.9%), fungal (20.3%), and bacterial (17.7%) necromass carbon. Regarding the SCMR, fungal-to-bacterial necromass ratio (16.6%), syringyl phenol (15.3%), vanillyl phenol (14.8%), lignin phenol (11.9%), and cinnamyl phenol (9.9%) were the most influential factors.

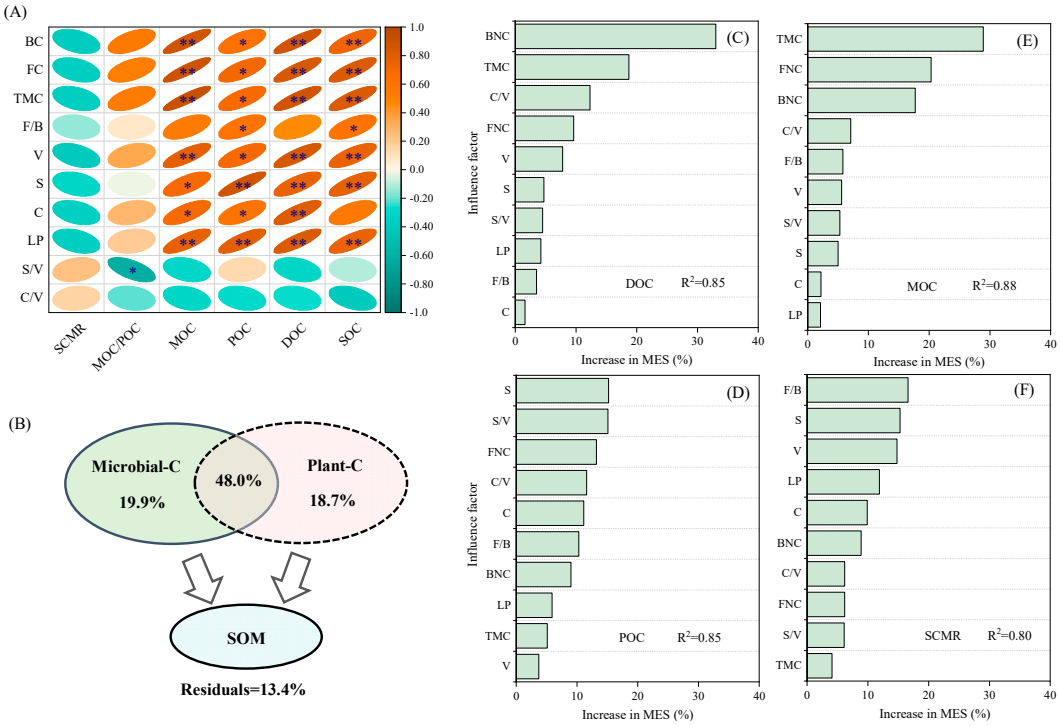


**Figure 6.** Effects of microbial necromass and lignin phenols on soil organic carbon fractions and stability ($n$ = 12). (**A**) Correlation heatmaps showing the relationship of soil microbial necromass and lignin phenols with soil organic carbon fractions and stability. (**B**) Variation partitioning analysis was used to assess the effects of soil microbial necromass and lignin phenols on soil organic carbon fraction. (**C**–**F**) The random forest model elucidated the relative significance of soil microbial necromass and lignin phenols to soil organic carbon fraction and stability. * $p < 0.05$, ** $p < 0.01$. BNC: bacteria necromass carbon; FNC: fungal necromass carbon; TMC: total microbial necromass carbon; V: vanillyl phenol; S: syringyl phenol; C: cinnamyl phenol; LP: lignin phenol; S/V: syringyl-to-vanillyl phenol ratio; C/V: cinnamyl-to-vanillyl phenol ratio. DOC: dissolved organic carbon; POC: particulate organic carbon; MOC: mineral-associated organic carbon; SCMR: soil carbon mineral rate; Microbial-C: including bacterial necromass carbon, fungal necromass carbon, microbial necromass carbon, and fungal-to-bacterial necromass carbon ratio; Plant-C: including vanillyl phenol, syringyl phenol, cinnamyl phenol, lignin phenol, syringyl-to-vanillyl, and cinnamyl-to-vanillyl phenol ratios. SOM: including soil organic carbon, dissolved organic carbon, particulate organic carbon, mineral-associated organic carbon.

## 4. Discussion

### *4.1. Effect of Straw Returning and Manure on Microbial Necromass and Lignin Phenol*

The long-term application of straw returning and manure (CS, CM, and CMS) significantly increased soil bacteria, fungi, and microbial necromass carbon compared to using only chemical fertilizers (CF) (Figure 2). This is because organic amendments boosted soil nutrients (Table S2), and stimulated microbial growth (Figure 4), speeding up microbial metabolism and increasing necromass carbon from bacteria and fungi. The decomposition of plant residues by soil microorganisms initiates rapid necromass formation, with microbial necromass becoming integral components of SOC [25]. Xu et al. [26] demonstrated that persistent organic amendments substantially increased subsoil microbial necromass

carbon, promoting soil carbon sequestration. The characteristics of substrates play a crucial role in determining the efficiency of converting organic materials into microbial necromass carbon [27], with variations in the composition of organic inputs differentially affecting microbial dynamics. The study revealed a slightly higher accumulation of bacterial and fungal necromass carbon in soils amended with manure (CM) compared to those amended with straw (CS) (Figure 2). This difference was likely attributable to the lower C:N ratio and increased nutrient bioavailability in manure, which promoted microbial proliferation. In contrast, the lignocellulosic composition of straw, characterized by higher C:N ratios, resulted in slower decomposition kinetics [28]. Notably, the CMS treatment exhibited greater microbial necromass carbon accumulation than the CS and CM amendments (Figure 2). This enhancement was attributed to the synergistic effects of combined organic inputs, which increased carbon diversity, improved microbial PLFAs (Figure 4), and stimulated enzymatic activity (Table 1). These findings are supported by Liu et al. [29], who demonstrated that incorporating animal manure with corn straw in agricultural fields markedly elevates soil microbial necromass carbon.

Fertilization regimes exerted a significant impact on soil lignin phenolic monomer, with CMS treatments demonstrating the highest accumulation of monomers (Figure 3). The combination of straw and manure enhanced soil nutrient availability (Table S1), thereby stimulating crop growth, increasing root exudate production (e.g., phenolic acids), and accumulating root stubble residues, which collectively contributed to elevated soil lignin phenolic content. Moreover, long-term manure application supplied labile carbon substrates that were preferentially metabolized by microorganisms [30], leading to the preservation of recalcitrant carbon and potentially facilitating lignin phenol accumulation in the CMS treatment. Liu et al. [29] also demonstrated that long-term application of organic fertilizer facilitated the microbial processing of lignin side-chains, while also promoting the stabilization of phenolics through humification processes. Microbial degradation of lignin generates phenolic derivatives, such as p-hydroxybenzoic and vanillic acids, which subsequently formed stable phenolic–protein complexes via humification and Maillard reactions [31]. This mechanism accounted for the observed accumulation of vanillyl, syringyl, and cinnamyl derivatives in the CMS treatment (Figure 3).

### *4.2. Effect of Microbial Necromass and Lignin Phenol on SOC Fraction*

Manure and straw application increase SOC by stimulating microbial activity and promoting the formation of diverse carbon compounds. This study revealed distinct variation in SOC components across the CM, CS, and CMS treatments, with CMS exhibiting the highest levels of SOC, DOC, POC, and MOC (Figure 1). This enhancement resulted from the synergistic mechanisms between organic amendments and straw. Manure supplies labile carbon substrates and essential nutrients, whereas straw offers structural carbon characterized by elevated carbon-to-nitrogen ratios. The concurrent application of these materials mitigates microbial nitrogen limitations during decomposition, and enhances the efficiency of carbon sequestration. Notably, the CMS treatment exhibited significantly reduced carbon mineralization rates compared to the application of single amendments (Figure 1F), thereby confirming improved carbon accumulation and stabilization through the strategy of co-application.

The distribution patterns of SOC fractions (DOC, POC, and MOC) demonstrated significant correlations with microbial necromass and lignin phenols (Figure 6B). According to the random forest model, bacterial necromass carbon and total microbial necromass carbon predominantly affected DOC levels (Figure 6C), potentially due to the release of soluble metabolites during microbial biomass turnover [32]. The POC was influenced by specific lignin biomarkers, namely syringyl and cinnamyl phenols, as well as fungal

necromass carbon (Figure 6D), indicating its composition of partially decomposed organic amendments. The structural complexity of lignin polymers, as indicated by lower syringyl-to-vanillyl and cinnamyl-to-vanillyl phenol ratios in the CMS treatment, likely contributed to enhanced POC retention by reducing its susceptibility to degradation.

For POC, syringyl phenol, cinnamyl phenol, fungal necromass carbon, as well as the syringyl-to-vanillyl and cinnamyl-to-vanillyl ratios, played critical roles in shaping its composition and distribution (Figure 6D). This was attributed to the fact that POC primarily comprises undegraded or partially decomposed organic matter. Lignin phenols, which are decomposition products of plant residues, exhibit complex structures and strong resistance to degradation, potentially allowing them to be more retained in POC. Consequently, the syringyl-to-vanillyl and cinnamyl-to-vanillyl phenols ratios can serve as indirect indicators of the decomposition extent of POC. The higher POC content observed in the CMS treatment may be explained by its lower syringyl-to-vanillyl and cinnamyl-to-vanillyl ratios, reflecting the recalcitrant characteristics of lignin.

The formation of MOC was primarily driven by microbial necromass components (Figure 6E). This necromass, comprising remnants of deceased microorganisms, includes stable components such as amino sugars and peptidoglycan that significantly contribute to MOC accumulation [33,34]. The interactions between microbial biomolecules, which possess positively charged amino groups, and soil minerals are charge-mediated and facilitate the formation of organo-mineral complexes [35]. Although plant-derived compounds such as lignin can contribute to MOC formation through hydrophobic interactions [36,37], their role appeared to be less significant compared to that of microbial-derived precursors [38,39]. Long-term organic fertilization enhanced MOC formation through several mechanisms: it increased microbial necromass production, promoted organo-mineral associations—especially those involving iron-bound complexes—and improved mineral availability for carbon stabilization [40,41]. These processes collectively accounted for the increased SOC sequestration capacity observed in integrated amendment practices.

### *4.3. Effect of Microbial Necromass and Lignin Phenol on SOC Mineraliation Rates*

The SOC mineralization rates were observed to be lowest in the CMS and CM treatments when compared to CF, CS, and CM treatments (Figure 1F). This finding suggested that the manure combined with straw incorporation enhanced the stability of SOC more effectively than treatments involving either manure or straw alone. These results are consistent with the findings of Huang et al. (2024) [42], which demonstrated that sustained organic amendments significantly enhanced SOC stability and sequestration by alleviating microbial nitrogen limitations and improving soil aggregation. The nitrogen derived from manure effectively alleviated the microbial nitrogen limitations caused by the high C:N ratio of straw, thereby promoting efficient microbial carbon metabolism. This biological process facilitated the accumulation of microbial byproducts, particularly polysaccharides and lipid complexes, which serve as essential precursors for stabilized organic carbon [43]. Simultaneously, this integrated approach accelerated the humification process of straw, wherein recalcitrant components like lignin undergo oxidation and condensation reactions under microbial influence [44], resulting in the formation of humic acid and humin. These compounds possessed intricate aromatic structures with high chemical stability, enabling their prolonged persistence in soil. Moreover, cementing agents in organic fertilizers, including polysaccharides and proteins, as well as decomposition products from straw, acted synergistically to promote soil particle aggregation, thereby facilitating the formation of macroaggregates (>250 μm) (Table S2). These aggregates encapsulated organic carbon, protecting it from microbial degradation and enzymatic activity, which in turn reduced decomposition rates.

The random forest model identified the fungal-to-bacterial necromass ratio and lignin phenol monomers as key determinants of the SOC mineralization rate (Figure 6F). Through the application of the random forest model, we identified that the primary determinants of SOC mineralization rate were the fungal-to-bacterial necromass ratio, as well as lignin phenols and their monomers (Figure 6F). The observed inverse relationship between SOC mineralization rate and fungal-to-bacterial necromass ratio (Figure 6A) underscored the pivotal role of fungal dominance in SOC stability. The cellular architecture of fungi, predominantly composed of chitin-melanin complexes and recalcitrant polysaccharides [43], provides chemically stable substrates rich in aromatic constituents that are resistant to enzymatic degradation. Fungal enzymatic systems facilitate the conversion of lignocellulose into aromatic humic polymers, thereby enhancing the chemical stability of SOC [45]. In contrast, bacterial biomass, which primarily consists of peptidoglycan (nitrogen-rich biopolymers), is more susceptible to rapid biodegradation. Although bacterial extracellular polysaccharides contribute to aggregate formation, their carbon matrices remain vulnerable to mineralization [46]. Fungal networks play a crucial role in the formation of macroaggregates by intertwining hyphae and secreting extracellular compounds such as glomalin proteins, which effectively encapsulate particulate organic matter within aggregate matrices [47]. Zhang et al. [9] have shown that fungal necromass were preferentially localized within aggregates, in contrast to bacterial remnants, which were more susceptible to decomposition due to soil moisture fluctuations and disruption from tillage. Consequently, higher fungal-to-bacterial necromass ratios enhanced physical protection mechanisms, thereby prolonging the residence time of SOC.

Another significant factor influencing the SOC mineralization rate was the presence of lignin phenols and their monomers, which exhibited a negative correlation with SOC mineralization rate (Figure 6A). This finding suggested that increased concentrations of lignin phenols may enhance SOC preservation through two primary mechanisms. Firstly, oxidative byproducts resulting from lignin degradation function as natural adhesives, chemically interacting with mineral surfaces such as clay particles to enhance soil aggregation and structural integrity [38,48]. Secondly, these aromatic compounds serve as chemically stable carbon reservoirs due to their inherent resistance to microbial degradation, thereby facilitating prolonged carbon storage and increasing SOC levels [49]. Importantly, POM was found to contain substantial amounts of lignin derivatives [50], indicating its crucial role in SOC stability through simultaneous physical protection within aggregates and chemical bonding with mineral surfaces during the decomposition of plant residues [51]. Overall, it is reasonable to conclude that long-term application of manure combined with straw returning not only increased the microbial necromass and lignin phenol contents but also improved the macroaggregate formation and thus contributed to SOC stability. It is crucial to emphasize that, although these results provided valuable insights into the relevant phenomena occurring in Calcaric-Fluvic Cambisols, other soil types, such as acidic, sandy, or clay soils, may demonstrate significantly different reaction mechanisms. To formulate more generalized conclusions, future research should aim to extend investigations to encompass a wider array of soil environments. This approach would not only enhance the applicability of the research findings but also provide more robust support for global soil management strategies (Figure 7).

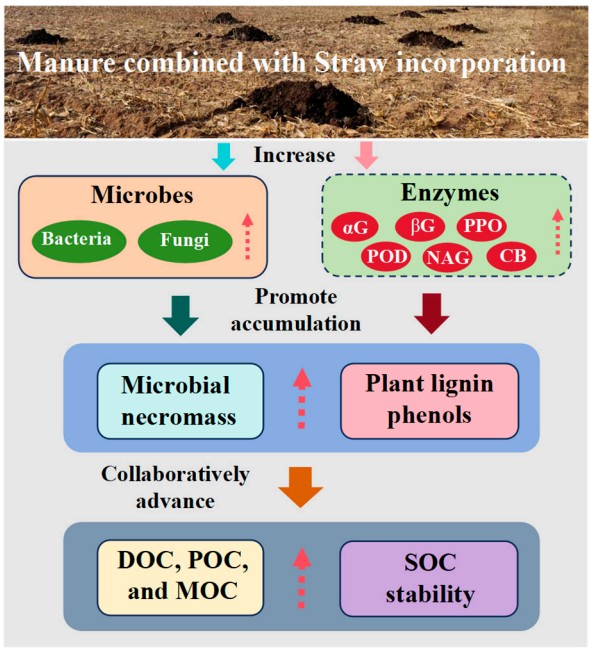


**Figure 7.** Conceptual diagram of the accumulation and contribution of microbial necromass carbon and lignin phenols to SOC fraction and stability under manure combined with straw incorporation. αG: α-glucosidase; βG: β-glucosidase; PPO: polyphenol oxidase; CB: cellobiohydrolase; POD: peroxidase; NAG: N-acetyl-β-D-glucosidase; SOC: soil organic carbon; DOC: dissolved organic carbon; POC: particulate organic carbon; MOC: mineral-associated organic carbon. The upward arrow along the dotted line indicates an upward trend.

## 5. Conclusions

A 17-year agricultural field study investigated the effects of long-term application of manure combined with straw returning on microbial necromass and lignin phenols, and their contributions to SOC fractions and stability. This integrated fertilization approach outperformed individual applications, enhancing microbial biomass and enzymatic activity, which facilitated the accumulation of both microbial necromass and plant-origin phenolic compounds. As a result, this synergistic management strategy primarily built SOC fractions through the accelerated accumulation of microbial necromass and plant lignin phenols. Specifically, DOC and MOC were predominantly influenced by microbial necromass, whereas POC was mainly affected by plant lignin phenols. The enhanced SOC stability under the combined treatment was attributed to two main factors: optimized fungal-to-bacterial necromass ratio and increased lignin phenol concentrations. These findings offer mechanistic insights into sustainable soil management, demonstrating how integrated organic amendments concurrently regulate biological and biochemical processes to augment carbon sequestration potential.

**Supplementary Materials:** The following supporting information can be downloaded at https://www.mdpi.com/article/10.3390/agronomy15061424/s1, Methods S1: The methodology of the analysis of studied soils (total nitrogen, available phosphate, potassium, and soil water-field capacity); Figure S1: Layout plan of the experimental plot; Table S1: Phospholipid fatty acid (PLFA) biomarkers chosen to characterize microbial community composition; Table S2: Effect of different fertilization treatments on soil nutrients and aggregates.

**Author Contributions:** Conceptualization, Y.W.; methodology, Y.W.; software, Y.W. and X.L.; validation, N.Y. and Y.L.; formal analysis, Y.W.; investigation, J.Z.; resources, Y.W.; data curation, Y.W.; writing—original draft preparation, Y.W.; writing—review and editing, J.Z.; visualization, X.L., N.Y.,

and Y.L.; supervision, J.Z.; project administration, Y.W.; funding acquisition, Y.W. All authors have read and agreed to the published version of the manuscript.

**Funding:** This research was funded by the Foundation Research Project of Shanxi Province, grant number 202203021212413 and the Scientific and Technological Innovation Foundation of Shanxi Agricultural University (Ph.D. Research Startup), grant number 2021BQ130. The Central Government-Guided Science and Technology Development Fund Project of Shanxi Province, grant number YDZJSX2023B008.

**Data Availability Statement:** The original contributions presented in the study are included in the article/Supplementary Materials, further inquiries can be directed to the corresponding author.

**Conflicts of Interest:** The authors declare no conflicts of interest.

## References

1. Liang, C.; Amelung, W.; Lehmann, J.; Kästner, M. Quantitative assessment of microbial necromass contribution to soil organic matter. *Glob. Change Biol.* **2019**, *25*, 3578–3590. [CrossRef] [PubMed]
2. Kleber, M.; Eusterhues, K.; Keiluweit, M.; Mikutta, C.; Mikutta, R.; Nico, P.S. Chapter one—Mineral-organic associations: Formation, properties, and relevance in soil environments. *Adv. Agron.* **2015**, *130*, 1–140. [CrossRef]
3. Cotrufo, M.F.; Ranalli, M.G.; Haddix, M.L.; Six, J.; Lugato, E. Soil carbon storage informed by particulate and mineral-associated organic matter. *Nat. Geosci.* **2019**, *12*, 989–994. [CrossRef]
4. Kleber, M.; Bourg, I.C.; Coward, E.K.; Hansel, C.M.; Myneni, S.C.B.; Nunan, N. Dynamic interactions at the mineral-organic matter interface. *Nat. Rev. Earth Environ.* **2021**, *2*, 402–421. [CrossRef]
5. Huang, X.L.; Jia, Z.X.; Jiao, X.Y.; Wang, J.L.; Huang, X.F. Long-term manure applications to increase carbon sequestration and macroaggregate-stabilized carbon. *Soil Biol. Biochem.* **2022**, *174*, 108827. [CrossRef]
6. Zhang, H.; Li, X.; Zhou, J.; Wang, J.; Wang, L.; Yuan, J.; Xu, C.; Dong, Y.; Chen, Y.; Ai, Y.; et al. Combined application of chemical fertilizer and organic amendment improved soil quality in a wheat-sweet potato rotation system. *Agronomy* **2024**, *14*, 2160. [CrossRef]
7. Lavallee, J.M.; Soong, J.L.; Cotrufo, M.F. Conceptualizing soil organic matter into particulate and mineral-associated forms to address global change in the 21st century. *Glob. Change Biol.* **2020**, *26*, 261–273. [CrossRef]
8. Cao, Y.F.; Ding, J.Z.; Li, J.; Xin, Z.M.; Ren, S.; Wang, T. Necromass-derived soil organic carbon and its drivers at the global scale. *Soil Biol. Biochem.* **2023**, *181*, 109025. [CrossRef]
9. Zhang, Q.; Li, X.Y.; Liu, J.J.; Liu, J.Y.; Han, L.; Wang, X.; Liu, H.Y.; Xu, M.P.; Yang, G.H.; Ren, C.J.; et al. The contribution of microbial necromass carbon to soil organic carbon in soil aggregates. *Appl. Soil Ecol.* **2023**, *190*, 104985. [CrossRef]
10. Simpson, A.J.; Simpson, M.J.; Smith, E.; Kelleher, B.P. Microbially derived inputs to soil organic matter: Are current estimates too low? Environ. *Sci. Technol.* **2007**, *41*, 8070–8076. [CrossRef]
11. Zhou, T.R.; Fan, J.B.; Zhang, L.X.; Lv, Q.L.; Wang, T.H.; Meng, Y.S.; Hu, H.; Gao, H.X.; Wang, J.; Ren, X.Q.; et al. The accumulation of plant- and microbial-derived carbon and its contribution to soil organic carbon in reclaimed saline-sodic farmland. *Appl. Soil Ecol.* **2024**, *202*, 105558. [CrossRef]
12. Ma, T.; Yang, Z.Y.; Shi, B.W.; Gao, W.J.; Li, Y.F.; Zhu, J.X.; He, J.S. Phosphorus supply suppressed microbial necromass but stimulated plant lignin phenols accumulation in soils of alpine grassland on the Tibetan Plateau. *Geoderma* **2023**, *431*, 116376. [CrossRef]
13. Lei, K.; Dai, W.; Wang, J.; Li, Z.; Cheng, Y.; Jiang, Y.; Yin, W.; Wang, X.; Song, X.; Tang, Q. Biochar and straw amendments over a decade divergently alter soil organic carbon accumulation pathways. *Agronomy* **2024**, *14*, 2176. [CrossRef]
14. Yu, Y.L.; Zhu, N.X.; Ren, Y.; Dong, M.H.; Sun, G.F.; Virk, A.L.; Li, F.M.; Yang, H.S.; Kan, Z.R. Effects of crop rotation on plant- and microbial-derived carbon within particulate and mineral fractions in paddy soils. *Agric. Ecosyst. Environ.* **2025**, *380*, 109398. [CrossRef]
15. Liu, L.; Yang, J.J.; Wang, J.; Yu, Q.; Wei, C.Z.; Jiang, L.C.; Huang, J.H.; Zhang, Y.H.; Jiang, Y.; Zhang, H.Y.; et al. Increase in mineral-associated organic carbon does not offset the decrease in particulate organic carbon under long-term nitrogen enrichment in a steppe ecosystem. *Soil Biol. Biochem.* **2025**, *202*, 109695. [CrossRef]
16. Meng, X.T.; Zhang, X.C.; Li, Y.N.; Jiao, Y.P.; Fan, L.C.; Jiang, Y.J.; Qu, C.Y.; Filimonenko, E.; Jiang, Y.H.; Tian, X.H.; et al. Nitrogen fertilizer builds soil organic carbon under straw return mainly via microbial necromass formation. *Soil Biol. Biochem.* **2024**, *188*, 109223. [CrossRef]
17. Li, J.N.; Zhao, J.; Liao, X.H.; Hu, P.L.; Wang, W.Y.; Ling, Q.M.; Xie, L.; Xiao, J.; Zhang, W.; Wang, K.L. Pathways of soil organic carbon accumulation are related to microbial life history strategies in fertilized agroecosystems. *Sci. Total Environ.* **2024**, *927*, 172191. [CrossRef]

18. Huang, J.; Ebach, M.C.; Triantafilis, J. Cladistic analysis of Chinese soil taxonomy. *Geoderma Reg.* **2017**, *10*, 11–20. [CrossRef]
19. Zhang, X.; Amelung, W. Gas chromatographic determination of muramic acid, glucosamine, mannosamine, and galactosamine in soils. *Soil Biol. Biochem.* **1996**, *28*, 1201–1206. [CrossRef]
20. Feng, X.; Nielsen, L.L.; Simpson, M.J. Responses of soil organic matter and microorganisms to freeze-thaw cycles. *Soil Biol. Biochem.* **2007**, *39*, 2027–2037. [CrossRef]
21. Gao, Q.Q.; Wang, L.H.; Fang, Y.Y.; Gao, Y.; Ma, L.X.; Wang, X.; Li, Y.Y.; Wu, X.P.; Du, Z.L. Conservation agriculture boosts topsoil organic matter by restoring free lipids and lignin phenols biomarkers in distinct fractions. *Soil Till. Res.* **2025**, *248*, 106463. [CrossRef]
22. Wen, Y.; Tang, Y.; Wen, J.; Wang, Q.; Bai, L.; Wang, Y.; Su, S.; Wu, C.; Lv, J.; Zeng, X. Variation of intra-aggregate organic carbon affects aggregate formation and stability during organic manure fertilization in a fluvo-aquic soil. *Soil Use Manage.* **2021**, *37*, 151–163. [CrossRef]
23. Zhang, J.; Zhang, F.; Yang, L. Continuous straw returning enhances the carbon sequestration potential of soil aggregates by altering the quality and stability of organic carbon. *J. Environ. Manag.* **2024**, *358*, 120903. [CrossRef]
24. Breiman, L. Random Forests. *Mach. Learn.* **2001**, *45*, 5–32. [CrossRef]
25. Chang, Y.; Sokol, N.W.; van Groenigen, K.J.; Bradford, M.A.; Ji, D.C.; Crowther, T.W.; Liang, C.; Luo, Y.Q.; Kuzyakov, Y.; Wang, J.K.; et al. A stoichiometric approach to estimate sources of mineral-associated soil organic matter. *Glob. Change Biol.* **2024**, *30*, 17092. [CrossRef]
26. Xu, Y.N.; Yu, Y.L.; Sheng, J.; Wang, Y.K.; Yang, H.S.; Li, F.M.; Liu, S.P.; Kan, Z.R. Long-term residue returning increased subsoil carbon quality in a rice-wheat cropping system. *J. Environ. Manag.* **2024**, *360*, 121088. [CrossRef] [PubMed]
27. Li, J.J.; Dong, L.B.; Fan, M.C.; Shangguan, Z.P. Long-term vegetation restoration promotes lignin phenol preservation and microbial anabolism in forest plantations: Implications for soil organic carbon dynamics. *Sci. Total Environ.* **2024**, *928*, 172635. [CrossRef]
28. Yang, S.S.; Sun, J.Y.; Wang, C.; Li, S.Y.; Li, Z.B.; Luo, W.; Wei, G.H.; Chen, W.M. Residue quality drives SOC sequestration by altering microbial taxonomic composition and ecophysiological function in desert ecosystem. *Environ. Res.* **2024**, *250*, 118518. [CrossRef] [PubMed]
29. Liu, X.; Bol, R.; An, T.T.; Liu, Y.C.; Xu, Y.D.; Li, S.Y.; Wang, J.K. Divergent accumulation of microbial necromass and plant lignin phenol induced by adding maize straw to fertilized soils. *Soil Till. Res.* **2024**, *243*, 106177. [CrossRef]
30. Li, Y.; Zhang, W.; Li, J.; Zhou, F.; Liang, X.; Zhu, X.; He, H.; Zhang, X. Complementation between microbial necromass and plant debris governs the longterm build-up of the soil organic carbon pool in conservation agriculture. *Soil Biol. Biochem.* **2023**, *178*, 108963. [CrossRef]
31. Wang, N.; Cui, Y.; Zhou, Y.; Liu, P.X.; Wang, M.S.; Sun, H.H.; Huang, Y.B.; Wang, S. Changes in the glucose concentration affect the formation of humic-like substances in polyphenol-maillard reactions involving gibbsite. *Molecules* **2024**, *29*, 2115. [CrossRef] [PubMed]
32. Wang, B.R.; An, S.S.; Liang, C.; Liu, Y.; Kuzyakov, Y. Microbial necromass as the source of soil organic carbon in global ecosystems. *Soil Biol. Biochem.* **2021**, *162*, 108422. [CrossRef]
33. Li, Z.; Duan, X.; Guo, X.B.; Gao, W.; Li, Y.; Zhou, P.; Zhu, Q.H.; O'Donnell, A.G.; Dai, K.; Wu, J.S. Microbial metabolic capacity regulates the accrual of mineral-associated organic carbon in subtropical paddy soils. *Soil Biol. Biochem.* **2024**, *195*, 109457. [CrossRef]
34. Zhang, X.W.; Wang, H.N.; Liu, Y.; Dong, H.L. Effect of clay mineral on bacteria-virus interactions and the fate of microbial biomass carbon. *Geochim. Et Cosmochim. Acta* **2025**, *394*, 383–392. [CrossRef]
35. Angst, G.; Mueller, K.E.; Nierop, K.G.J.; Simpson, M.J. Plant-or microbial-derived? A review on the molecular composition of stabilized soil organic matter. *Soil Biol. Biochem.* **2021**, *156*, 108189. [CrossRef]
36. Mikutta, R.; Turner, S.; Schippers, A.; Gentsch, N.; Meyer-Stüve, S.; Condron, L.M.; Peltzer, D.A.; Richardson, S.J.; Eger, A.; Hempel, G.; et al. Microbial and abiotic controls on mineral-associated organic matter in soil profiles along an ecosystem gradient. *Sci. Rep.* **2019**, *9*, 10294. [CrossRef]
37. Hu, Q.Y.; Zhang, X.L.; Zhang, Z.W.; Wang, R.F.; Feng, C.; Xie, Y.X.; Chen, S.J.; Liu, T.Q. Microbial inoculants addition increases microbial necromass but decreases plant lignin contribution to soil organic carbon in rice paddies. *Soil Till. Res.* **2025**, *250*, 106529. [CrossRef]
38. Keller, A.B.; Borer, E.T.; Collins, S.L.; DeLancey, L.C.; Fay, P.A.; Hofmockel, K.S.; Leakey, A.D.B.; Mayes, M.A.; Seabloom, E.W.; Walter, C.A.; et al. Soil carbon stocks in temperate grasslands differ strongly across sites but are insensitive to decade-long fertilization. *Glob. Change Biol.* **2022**, *28*, 1659–1677. [CrossRef]
39. Underwood, T.R.; Bourg, I.C.; Rosso, K.M. Mineral-associated organic matter is heterogeneous and structured by hydrophobic, charged, and polar interactions. *Proc. Natl. Acad. Sci. USA* **2024**, *121*, e2413216121. [CrossRef]
40. Xu, Y.; Sheng, J.; Zhang, L.P.; Sun, G.F.; Zheng, J.C. Organic fertilizer substitution increased soil organic carbon through the association of microbial necromass C with iron oxides. *Soil Till. Res.* **2025**, *248*, 106402. [CrossRef]

41. Huang, X.; Jia, Z.; Guo, J.; Li, T.; Sun, D.; Meng, H.; Yu, G.; He, X.; Ran, W.; Zhang, S.; et al. Ten-year long-term organic fertilization enhances carbon sequestration and calcium-mediated stabilization of aggregate-associated organic carbon in a reclaimed *Cambisol*. *Geoderma* **2019**, *355*, 113880. [CrossRef]
42. Huang, X.L.; Li, Y.Y.; Zhang, D.D.; Zhao, Y.; Wang, Y.; Liu, Q.X.; Dong, E.W.; Wang, J.S.; Jiao, X.Y. Long-term organic fertilization combined with deep ploughing enhances carbon sequestration in a rainfed sorghum-maize rotation system. *Geoderma* **2024**, *442*, 116778. [CrossRef]
43. Yang, J.J.; Li, A.Y.; Yang, Y.F.; Li, G.H.; Zhang, F. Soil organic carbon stability under natural and anthropogenic-induced perturbations. *Earth Sci. Rev.* **2020**, *205*, 103199. [CrossRef]
44. Dong, S.; Li, R.; Zhou, K.; Wei, Y.; Li, J.; Cheng, M.; Chen, P.; Hu, X. Response of humification process to fungal inoculant in corn straw composting with two different kinds of nitrogen sources. *Sci. Total Environ.* **2024**, *946*, 174461. [CrossRef] [PubMed]
45. Su, Q.Y.; Wu, Y.; Wang, S.Y.; Li, Y.R.; Zhao, J.H.; Huang, F.L.; Wu, J.Q. The reverse function of lignin-degrading enzymes: The polymerization ability to promote the formation of humic substances in domesticated composting. *Bioresour. Technol.* **2023**, *380*, 129059. [CrossRef]
46. Costa, O.Y.A.; Raaijmakers, J.M.; Kuramae1, E.E. Microbial extracellular polymeric substances: Ecological function and impact on soil aggregation. *Front. Microbiol.* **2018**, *9*, 1636. [CrossRef] [PubMed]
47. Ji, L.L.; Chen, X.H.; Huang, C.Q.; Tan, W.F. Arbuscular mycorrhizal hyphal networks and glomalin-related soil protein jointly promote soil aggregation and alter aggregate hierarchy in Calcaric Regosol. *Geoderma* **2024**, *452*, 117096. [CrossRef]
48. Zhu, S.; Dai, G.; Ma, T.; Chen, L.; Chen, D.; Lv, X.; Wang, X.; Zhu, J.; Zhang, Y.; Bai, Y.; et al. Distribution of lignin phenols in comparison with plant-derived lipids in the alpine versus temperate grassland soils. *Plant Soil* **2019**, *439*, 325–338. [CrossRef]
49. Li, Z.; Wei, X.M.; Zhu, Z.K.; Fang, Y.Y.; Yuan, H.Z.; Li, Y.H.; Zhu, Q.H.; Guo, X.B.; Wu, J.S.; Kuzyakov, Y.; et al. Organic fertilizers incorporation increased microbial necromass accumulation more than mineral fertilization in paddy soil via altering microbial traits. *Appl. Soil Ecol.* **2024**, *193*, 105137. [CrossRef]
50. Zhang, J.J.; Lei, L.; Xiao, W.F.; Yang, X.; Horwath, W.R.; Liao, Y.L.; Yang, H.B.; Jian, Z.J.; Zeng, L.X. Vetch cover crops increase particulate organic carbon in citrus orchard by increasing lignin phenols. *Appl. Soil Ecol.* **2025**, *207*, 105921. [CrossRef]
51. Witzgall, K.; Vidal, A.; Schubert, D.I.; Höschen, C.; Schweizer, S.A.; Buegger, F.; Pouteau, V.; Chenu, C.; Mueller, C.W. Particulate organic matter as a functional soil component for persistent soil organic carbon. *Nat. Commun.* **2021**, *12*, 4115. [CrossRef] [PubMed]